Component Terminal Dynamics in Poly(ethylene oxide)/Poly(methyl methacrylate) Blends

Ilan Zeroni,[†] Sahban Ozair,[†] and Timothy P. Lodge*[,†,‡]

Department of Chemical Engineering and Materials Science, University of Minnesota, Minneapolis, Minnesota 55455, and Department of Chemistry, University of Minnesota, Minneapolis, Minnesota 55455

Received April 28, 2007; Revised Manuscript Received April 9, 2008

ABSTRACT: The rheological response of high molecular weight tracer chains of poly(ethylene oxide) (PEO) and poly(methyl methacrylate) (PMMA), separately blended with low molecular weight PEO/PMMA matrices of varying composition, were obtained over a 120 deg temperature window. Monomer friction factors, ζ, for each component as a function of temperature and matrix composition were extracted by various means, all of which yielded consistent results. The tracer diffusivities of low molecular weight PEO chains in some of the same blends were obtained by forced Rayleigh scattering, and the resulting friction factors agree well with those obtained using rheology. The overall results show that the mobilities of both PMMA and PEO are strongly composition-dependent in PMMA-rich blends, their monomeric friction factors dropping precipitously upon addition of small amounts of PEO. The composition dependence of the PMMA ζ is strong over a wide composition range, whereas that of PEO is only significant at high PMMA content blends. Friction factors for the PEO component are significantly larger than those inferred from segmental dynamics measurements reported in the literature. The Lodge−McLeish self-concentration model, as usually applied, is unable to predict the observed behavior of either component. However, the data can be nearly quantitatively described using a simple but empirical mixing rule. Selected experiments were repeated using a PEO matrix with methoxyl rather than hydroxyl end groups; except for the change in glass transition temperature for the PEO, no significant effects were observed.

Introduction

Miscible binary polymer blends exhibit some interesting phenomena that challenge our understanding of polymer dynamics. These include widening of the calorimetric glass transition temperature[1,2] (or even resolution of two distinct transitions[3]) and failure of time−temperature superposition.[4–6] The former has been traced to the distinct local environments experienced by segments in the blend, whereas the latter reflects the fact that the viscoelastic relaxation times of each species in the blend exhibit different temperature dependences.

A further complication that has recently emerged is a discrepancy between the temperature dependence of the segmental and terminal dynamics for a given component, even at temperatures significantly higher than the component glass transition temperature in the blend.[7,8] Blends of poly(ethylene oxide) (PEO) and poly(methyl methacrylate) (PMMA) exhibit this phenomenon strikingly.[7,9] For example, the monomeric friction factor (ζ_{PEO}) of a tracer PEO chain in a PMMA matrix, obtained via methods that measure terminal relaxation, can be as much as several orders of magnitude larger than that obtained via direct measurements of PEO segmental motion. This is so even tens of degrees above the glass transition of the PMMA matrix.[7] Moreover, it has been reported that this blend is exceptional in that the Lodge−McLeish "self-concentration" model[10] is not able to describe the PMMA results even approximately.[9] This system has been shown to be miscible[11] up to an LCST temperature of about 225 °C.[12]

Selected component terminal dynamics have been previously extracted for PEO/PMMA blends using forced Rayleigh scattering,[7] simultaneous infrared dichroism and flow birefringence following a linear step strain,[13] and rheology.[4,7] The data obtained via these methods are restricted in the available composition and/or temperature range. Other studies have examined various aspects of PEO/PMMA dynamics, but without resolving the separate components.[14–18] To date, there exists no complete set of component terminal dynamics data extending over a wide range of composition (ϕ) and temperature (T) for both components in PEO/PMMA mixtures. The aim of this work, therefore, is to explore the terminal dynamics of both components in the PEO/PMMA system, over the complete ϕ range and over as wide a T range as possible.

Rheological methods offer an appealingly simple route to extract component dynamics in a blend.[4,7,19–28] Several distinct approaches have been used, either in blends of different species or in molecular weight blends. One method relies on mixing two samples of such (high) molecular weights and glass transition temperatures that their longest relaxation times in the well-entangled blend can be resolved in the available frequency and temperature range. This method was utilized, for example, to extract the component terminal dynamics of PI/PVE blends over a wide temperature and composition range by fitting a double reptation model[29,30] to the dynamic moduli.[21] Another tactic is to disperse a high molecular weight tracer in a low molecular weight matrix, as used previously for PEO tracers in PMMA;[7] this is the main approach adopted here. A third method, recently applied to bimodal blends of PB, PI, and PS, mixes low molecular weight chains in a high molecular weight, highly entangled matrix.[27] Yet a further possibility is to apply mixing rules for the zero shear rate viscosity of blends.[31] Such models may be used to extract the contribution of a tracer to the overall viscosity of the blend, in turn affording the terminal dynamics of the tracer component.

The methodologies used here were adapted from a recent publication,[7] where 1% of a high molecular weight PEO sample was dissolved in modest molecular weight PMMA. The longest relaxation time of the tracer was extracted via low-frequency peaks in the elastic component of the dynamic viscosity, η'', yielding ζ_{PEO} via the Rouse model. In this work we dissolve small quantities of a high molecular weight tracer, either PEO

* Author for correspondence: e-mail lodge@umn.edu.
† Department of Chemical Engineering and Materials Science.
‡ Department of Chemistry.

10.1021/ma0709809 CCC: $40.75
Published on Web 06/04/2008

Table 1. Homopolymer Properties; WLF Constants Are Referenced to the Calorimetric T_g

sample	M_n (kDa)	M_w/M_n	rr/rm/mm	T_g (K)	C_1	C_2 (K)	ζ_0 (kg/s)
PEO-1	1.03[a,b]	1.03[a,b]		210	8.2	52.5	3.24×10^{-6}
PEO-900	898[d]	1.08[d]		213			
PEO DME-1	1.03[a]	1.02[a]		187[f]	9.4	48.7	2.88×10^{-5}
PMMA-1.5	1.54[a,c,e]	1.05[a,e]	73.3/26.7/0	329	16.8	76.7	1.80×10^{1}
PMMA-100	101	1.09	79.4/20.6/0	405			
PMMA-300	295	1.25		394			

[a] Obtained through MALDI-TOF analysis. [b] Excluding $m/z < 501$. [c] DP = 10 obtained via NMR end-group analysis. [d] According to certificate of analysis provided by manufacturer. [e] Excluding $m/z < 501$. [f] Literature value.[41]

or PMMA, in mixtures of low molecular weight PEO and PMMA and extract the component terminal dynamics from linear viscoelastic measurements. In the case of PEO, tracer diffusivities have also been obtained by forced Rayleigh scattering (FRS). The PEO friction factors extracted from rheology and FRS agree well. The T and ϕ dependences of the friction factors are then compared with the predictions of the Lodge−McLeish model, with empirical mixing rules, and with selected data in the literature.

Experimental Section

Materials. A high molecular weight PEO sample (PEO-900) was purchased from Polymer Laboratories. Low molecular weight PEO (PEO-1) and PEO dimethyl ether (PEO DME-1) samples were purchased from Aldrich. The numbers denote M_n of the sample in kDa. All samples have polydispersity indices lower than 1.1, according to the manufacturer (PEO-900) and MALDI-TOF analysis (PEO-1, PEO DME-1) using a Bruker Reflex III instrument in reflectron mode. The MALDI recipe used for PEO and PEO DME entailed 15 μL of a 20 mg/mL 1,8,9-anthracenetriol (dithranol) solution in THF, 2 μL of a 5 mg/mL sodium trifluoroacetate solution in THF, and 5 μL of a 10 mg/mL PEO or PEO DME solution in THF.

Three PMMA samples (PMMA-1.5, PMMA-100, and PMMA-300) were synthesized through anionic polymerization.[32–34] Methyl methacrylate (MMA), 1,1-diphenylethylene (DPE), and triethylaluminum (TEA) were purchased from Aldrich. Tetrahydrofuran was dried by passing through alumina columns. MMA was degassed over calcium hydride and allowed to stir for 48 h. MMA was distilled to a purification flask, and TEA was then added until the solution turned bright yellow, sustaining its color for several minutes. Some more TEA was then added.[35] The mass of the uninhibited MMA was determined by distillation to a tared burette. In order to prepare the initiator, degassed DPE was transferred to a vessel containing some THF, followed by *sec*-butyllithium. This solution was allowed to react for 1 h to form 1,1-diphenylhexyllithium (DPHL). The concentration of DPHL was determined using the Gilman double titration method.[36] THF was added to the reactor, cooled to −70 °C, and stirred vigorously. The DPHL solution was then transferred to the reactor. Having seen that the deep red color characteristic of DPHL had persisted for about 10 min, MMA was added dropwise while maintaining the temperature at −70 °C. Once all the monomer had dripped into the reactor, the solution was stirred for a further 15 min. A degassed solution of 5% acetic acid in methanol was then added to terminate the reaction. The high molecular weight PMMA was cleaned by removing the THF, redissolving in methylene chloride, water washing the solution three times, and precipitating into a 50:50 solution of methanol and isopropanol. The precipitate was dried in a vacuum oven heated to 40 °C for 5 days.

The low molecular weight PMMA was yellowish in color due to the high concentration of lithium salts. Removing the THF, redissolving in toluene, and precipitating into hexanes cleaned this polymer. The polymer became considerably whiter after each precipitation, and after three repeats of this procedure, the SEC refractometer peak that corresponds to the salts disappeared completely. Details of the SEC setup are found elsewhere.[21] The polymer was then dried in a vacuum oven heated to 40 °C for 5 days. The polydispersity of PMMA-100 and PMMA-1.5, as obtained by SEC (PMMA-100) and SEC and MALDI-TOF (PMMA-1.5), is less than 1.1. The polydispersity of PMMA-300, as obtained by SEC, is 1.25. Molecular weights were obtained by a light scattering detector (Wyatt Technology DAWN), and the refractive index increment, dn/dc, is 0.086 mL/g at 633 nm.[37]

The MALDI recipe used for PMMA is detailed elsewhere.[38] Sodium trifluoroacetate was the salt used in this study. The triad contents of the PMMA-1.5 and PMMA-100 samples were determined via 300 MHz, ^{1}H NMR using $CDCl_3$ as solvent with TMS as a reference. The rr and rm peaks were found at 0.78−0.92 and 0.92−1.08 ppm, respectively.[39] Generally, this method of synthesis provides PMMA samples with roughly 73−80% syndio and 20−27% hetero microstructures. The properties of all the polymers are detailed in Table 1. The tacticity results obtained are consistent with literature values for anionically synthesized PMMA initiated with similar compounds.[40]

Blends for the rheological measurements were prepared by codissolving the polymers in benzene, stirring the solution for 24 h, warming while stirring, and stirring the cooled solution for an additional 24 h. Benzene was then evaporated under nitrogen flow. Finally, the blends were dried in a vacuum oven heated to 40 °C for 5 days. The blend compositions were chosen to have the same mean monomer fraction, regardless of the tracer. For example, a 20% PMMA blend with a PMMA tracer actually comprises 19% low molecular weight PMMA and 1% high molecular weight PMMA. A 20% PMMA blend with a PEO tracer actually comprises 79% low molecular weight PEO and 1% high molecular weight PEO. The 100 kDa PMMA tracer was used throughout this work. The 300 kDa PMMA tracer was only blended with pure PEO to explore the dependence of these results on tracer molecular weight.

Methods. The rheometer used was the TA ARES LS2, equipped with a 2KFRTN1 force rebalance transducer featuring a 2×10^{-7} kg·m (1.96×10^{-6} kg·m^2/s^2 or kg force·m) lower torque limit. The transducer is regularly calibrated using the calibration kit provided with the instrument. Temperature was controlled via a convection oven using nitrogen. Either 50 or 7.9 mm diameter parallel plates were used. The latter were used for PMMA-rich samples at lower temperatures. Special care was taken to exclude bubbles from the sample while loading. Each sample was annealed at 100 °C while shearing at a moderate shear rate for at least 10 min before any further experiments were conducted. This allowed whatever small bubbles might still be present to flow to the center of the geometry, where their effect on the torque is minimal. At each temperature, the sample loading was checked visually, to ensure that the edge is flat. The thermal expansion of the stainless steel plates was determined to be 2.4 μm/K. Assuming linear expansion with temperature, the actual gap at each temperature was determined, and the data recalculated using the new value. All steady shear viscosity data were taken at several shear rates, spanning at least a decade, to ensure that a constant value is obtained at each temperature. Thus, it was confirmed that the viscosity throughout the parallel plates geometry is constant despite the radially nonhomogeneous shear rate. Because of its low viscosity, PEO was loaded on the stress-controlled TA RA2000ex rheometer, featuring a lower torque limit of $\sim 10^{-9}$ kg·m (10^{-8} kg force·m) for steady shear experiments. The Couette geometry was used in these experiments, and no corrections for thermal expansion of the

cup and bob were made. The results obtained agreed very well with those obtained for the same sample using the ARES.[7]

It is conceivable that annealing benzene-cast PEO/PMMA blends at 100 °C for 10 min may not be sufficient to attain equilibrium.[41] However, measurements at 100 °C at the beginning and end of the measurement series, where the temperature had been raised by 10 °C intervals to at least 140 °C and kept at each temperature for at least 10 min, yielded the same results. We are therefore satisfied that the samples were sufficiently annealed and were at equilibrium.

The experimental technique and setup of forced Rayleigh scattering are described elsewhere.[7,42] Poly(ethylene oxide) (PEO-1) was allowed to react with 4′-(*N,N*-dimethylamino)-2-nitrostilbene-4-carboxylic acid (ONS-COOH); the labeling reaction is described elsewhere.[7] The optically labeled PEO chains were used as tracers in the FRS experiments. Polymer blends were prepared by dissolving labeled PEO (1 wt %), unlabeled PEO, PMMA, and trace amounts of the antioxidant 2,6-di-*tert*-butyl-4-methylphenol (BHT) in methylene chloride. The solution was filtered, and the solvent was removed by evaporation. The sample was dried in a vacuum oven at a temperature of 150 °C until no weight change was observed. The FRS sample was prepared under argon by sealing the polymer blend with silicone adhesive between two glass disks, separated by a 1 mm thick aluminum spacer. The sealant was dried overnight to ensure a proper seal.

FRS decays were acquired for each blend at several grating spacings, d, for each temperature. The decays (scattered intensity, I, vs time, t) exhibited one relaxation mode and were fit using the following equation:

$$I(t) = \{A \exp[-(t/\tau)^{\beta}]\}^2 + I_b \quad (1)$$

A, β, and τ are fitting parameters, and I_b is the incoherent background. The extracted β values were in the range of 0.55−1.0, indicating the experimental decays were broader than a single-exponential decay. This broadening can be attributed primarily to a combination of experimental noise near the baseline and tracer polydispersity.[7] To account for the decay broadening, the mean relaxation time, $\langle\tau\rangle$, was determined using the following equation:

$$\langle\tau\rangle = \frac{\tau}{\beta}\Gamma\left(\frac{1}{\beta}\right) \quad (2)$$

where Γ is the gamma function. Once $\langle\tau\rangle$ is determined from FRS decay curves, it is used to calculate diffusion coefficient, D, of the labeled PEO chains using the following relationship:

$$\langle\tau\rangle = \frac{d^2}{4\pi^2 D} \quad (3)$$

For each composition, $\langle\tau\rangle$ was plotted as a function of d^2 for different temperatures. As expected, $\langle\tau\rangle$ varied linearly with d^2, confirming that the erasure of the optical grating is due to diffusion-controlled mechanisms only. Also plotted was $1/\langle\tau\rangle$ vs $1/d^2$, and the slope of the best-fit line in each plot was used to determine the diffusion coefficient. The reported data are calculated from the average of the two diffusion coefficients determined from $\langle\tau\rangle$ vs d^2 and $1/\langle\tau\rangle$ vs $1/d^2$ plots. The maximum, untypical deviation from the average is 17%. For most other data points, the deviation is smaller than 1%. The monomeric friction coefficient was calculated using eq 3 and the Rouse model relation $\zeta = k_B T/ND$, where k_B is Boltzmann's constant, T is absolute temperature, and N is the degree of polymerization.

Results

In this section, we describe four related methods used to extract component monomeric friction factors, ζ, from the rheological data. For the pure low molecular weight homopolymer melts, we used the zero shear viscosity η and the Rouse model to extract ζ. We present three more methods to extract ζ that apply to pure homopolymer melts as well as blends, using the three material functions η', η'', and η. The disparity in chain lengths between the matrix and tracer chains gives rise to distinct relaxation peaks in η'', two plateaus in the frequency dependence of η', and a blend viscosity that is measurably higher than that of the matrix. We attribute these phenomena to the contribution of the tracer chains in the blend and utilize simple formulations to extract the longest relaxation time of the tracer chain or the tracer contribution to η or η'. We then use Rouse model equations to extract the tracer component ζ from the longest relaxation time, but it is important to emphasize that this step only invokes an assumption about the molecular weight dependence of the tracer relaxation and does not affect the ϕ and T dependences that are the focus of the work. Furthermore, for the few cases where direct comparisons can be made between ζ thus extracted from tracers of different M, the results agree well.

Extracting ζ via Steady Shear Viscosity of the Pure Homopolymer Melt. We obtained the viscosity of the low molecular weight matrix components PMMA-1.5, PEO-1, and PEO DME-1. Since these polymers are not entangled, we use the Rouse model[43,44] to extract ζ:

$$\zeta = 36\frac{m_0}{\rho N_{av}}\frac{m_0}{b^2 M_n}\eta \quad (4)$$

where m_0 is the monomer molecular weight, ρ is the melt density (1130 kg/m^3 for PMMA and 1064 kg/m^3 for PEO and PEO DME[45]), N_{av} is Avogadro's number, M_n is the number-average molecular weight, and b is the statistical segment length (6.5 and 5.6 Å for PMMA and PEO, respectively[45]). These results are shown in Figure 1. The magnitude of ζ obtained via this method is systematically larger than that obtained via some of the following methods, FRS data, and literature data. The results obtained via the different methods come into better agreement when we divide the right-hand side of eq 4 by a factor of about 3. As the values of ζ range over many orders of magnitude with variations in T and ϕ, this correction is not significant. We speculate that this difference arises, at least in part, from the contribution of "glassy modes" to the viscosity of the short polymers.[46] As the viscosity is the time integral of the stress relaxation modulus and as the terminal dynamics of short chains are not much separated in time from the glassy modes, this contribution can be noticeable.

Extracting ζ via Peaks in η''. Under many conditions (ϕ,T) the presence of the high molecular weight tracer gave rise to a distinct peak in η'', which is attributable to the longest relaxation time of the tracer chains (see Figures 2 and 3). The plots shown in Figure 2 (PMMA tracer) and Figure 3 (PEO tracer) are collections of several data sets obtained at various temperatures. For the pure homopolymer melts, horizontal shift factors, a_T, were determined by overlapping tan δ. Vertical shift factors, b_T, were then determined by overlapping η' and η'' simultaneously. Indeed, not all of the data sets in these plots exhibit a clear η'' peak. The longest relaxation times for these temperatures were then deduced from the relaxation time at the reference temperature and the value of the horizontal shift factor. For the blends, the data sets in which the tracer relaxation peaks were evident were shifted horizontally such that the relaxation peaks overlapped. They were then shifted vertically such that η' would overlap. These are termed "peak overlap" data sets. An example of how this is different from the standard TTS procedure can be seen in Figure 3d,e, where after horizontal shifting η' and η'' cannot be overlapped simultaneously by a single vertical shift. These blends (PEO tracers in PMMA-rich matrices) show other unique features, as will be discussed subsequently. Data sets that did not exhibit the peak were shifted as previously described for the pure homopolymer melts, by matching the shapes of tan δ in the appropriate frequency range

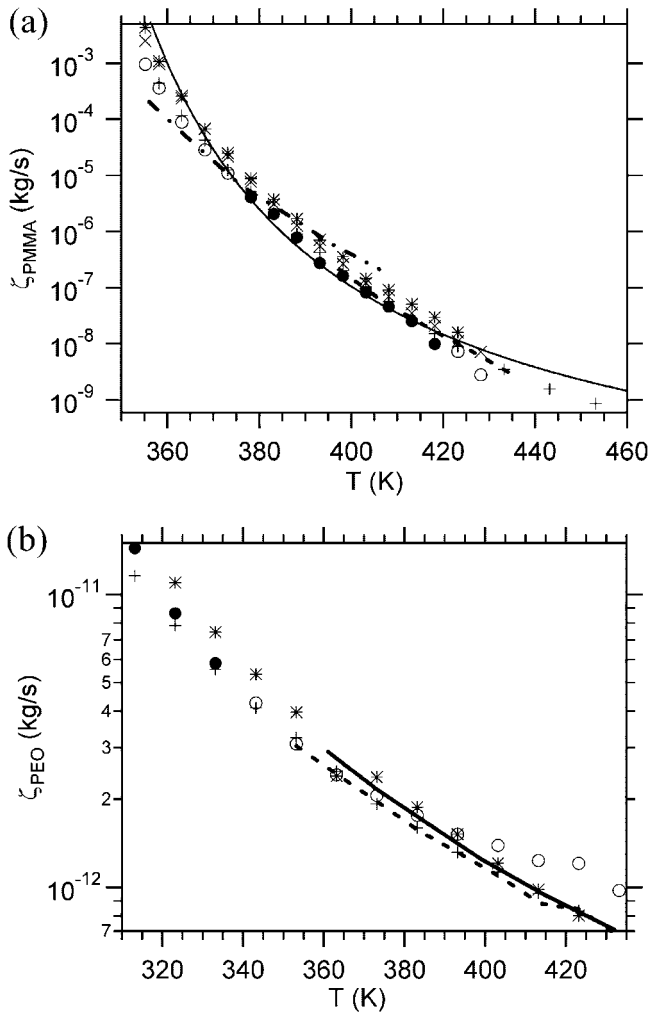

Figure 1. Monomeric friction factors of (a) 100 kDa PMMA in PMMA and (b) PEO in PEO, extracted via the various methods explained in the text, as well as literature data: (+) homopolymer viscosity; (●) longest relaxation time, peak overlap; (○) longest relaxation time, TTS; (×) tracer contribution to η'; (∗) tracer contribution to η. Data from the literature are shown as (a) a solid line (WLF fit to the data),[9] a dashed line,[48] and a dash-dot line[49] and (b) a solid line[50] and a dashed line.[7] Literature data were shifted horizontally by −55, −51, −68, 12, and 0 K, respectively, to account for T_g differences.

as if TTS were valid for these blends. The longest relaxation times for these temperatures were deduced from the relaxation time at the reference temperature and the value of the horizontal shift factor, as in the case of the pure homopolymer melts. These data sets are termed "TTS" data sets.

It is well-known that TTS is not generally valid in miscible blends. However, we are using it only in a very restricted sense, essentially to extend the T range over which relaxation data can be obtained for any given blend. Furthermore, upon inspection of Figures 2 and 3, one may see that at frequencies lower than that of the tracer chain relaxation peak TTS is valid, with perhaps the exception of PMMA in 90% PMMA (Figure 2d). This is because at such long times the matrix components have fully relaxed. These frequencies correspond to temperatures that are higher than those for which there is a prominent peak in η''. It is at frequencies higher than that of the tracer chain relaxation peak that TTS fails. These frequencies correspond to temperatures that are lower than those for which there is a prominent peak in η''. Nevertheless, Figures 1a and 4 show that the data obtained via this method agree well with the data obtained via the other methods even at low temperatures, and

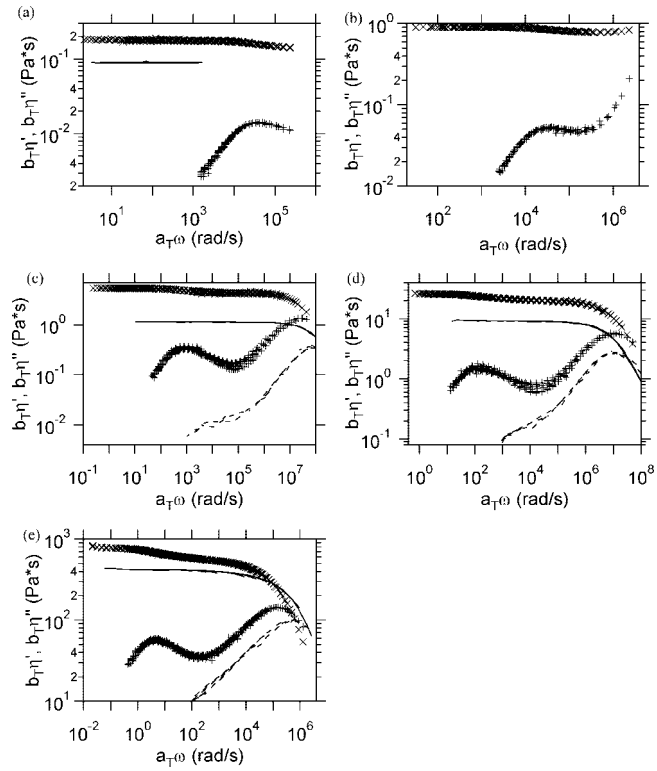

Figure 2. Complex shear viscosity components vs reduced frequency for PMMA-100 tracers in (a) 50% PMMA, (b) 64% PMMA, (c) 80% PMMA, (d) 90% PMMA, and (e) 100% PMMA. The reference temperature for all master curves is 130 °C. (×) $-\eta'$; (+) $-\eta''$. Solid and dashed lines are η' and η'' of the matrix blends, respectively.

we therefore consider these low-temperature "TTS" data sets to provide reasonable estimates of ζ(T).

Once the longest relaxation times of the tracer chains had been obtained, the monomeric friction factors of the tracer chains were calculated using the Rouse model:[43,47]

$$\zeta = 3\pi^2 k_B T \frac{m_0}{M_n} \frac{m_0}{b^2 M_n} \tau_1 \tag{5}$$

where τ_1 is the longest relaxation time. The use of eq 5 is really only a means to convert a measured longest relaxation time into a friction factor. As note above, it does not modify the ϕ or T dependences in any way. Furthermore, as almost all of the data for each polymer were extracted from a single M, the assumed Rouse dependence is not central to the results. This is not to say that the M dependence is not interesting in its own right, but that will be addressed in a subsequent report.

Extracting ζ via Steady Shear Viscosity of Tracer Blends. The key assumption in this analysis is that any difference between the steady shear viscosity of a tracer blend and that of its matrix is due to the additive contribution of the tracer chains. We then formulate a simple relation

$$\eta_{blend} = \phi_{matrix}\eta_{matrix} + (\phi_{tracer} + A\phi_{tracer}^2)\eta_{tracer} \tag{6}$$

where ϕ_i is the volume fraction of i. Extracting η_{tracer} from eq 6 allows us to obtain the tracer monomeric friction factor via eq 4. We divide the RHS of eq 4 by a factor of 3 as we did with the homopolymer viscosity data. The density used in eq 4 is the matrix density, estimated by interpolation of the homopolymer densities. All other parameters used in eq 4 pertain to the tracer. We found good agreement between data obtained via this and other methods when $A_{PMMA} = -20$ and $A_{PEO} = -30$ (see Figures 4 and 5). The simplest method of extracting the dissipative contribution of a viscoelastic element in dilute

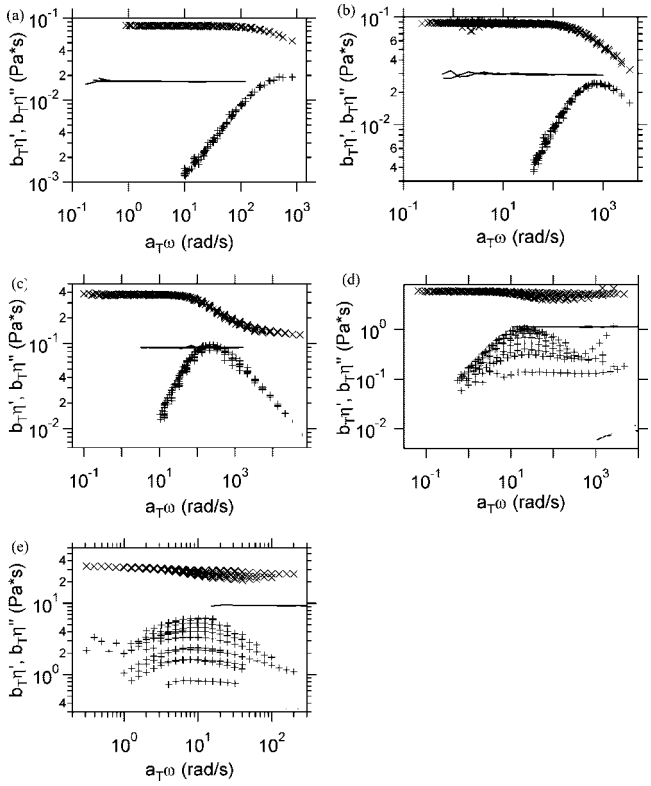

Figure 3. Complex shear viscosity components vs reduced frequency for PEO tracer in (a) 0% PMMA, (b) 20% PMMA, (c) 50% PMMA, (d) 80% PMMA, and (e) 90% PMMA. The reference temperature for all master curves is 130 °C. (×) $-\eta'$; (+) $-\eta''$. Solid and dashed lines are η' and η'' of the matrix blends, respectively.

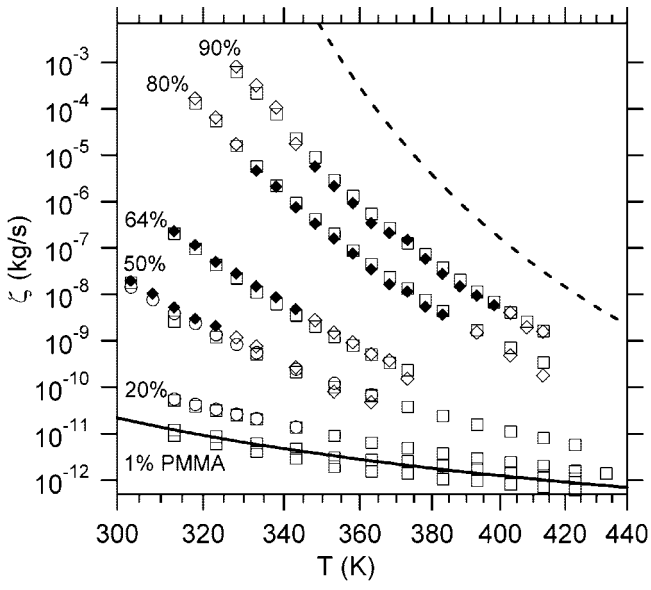

Figure 4. Monomeric friction factors of PMMA in PEO/PMMA blends. Solid and dashed lines are PEO and PMMA homopolyimer WLF fits, respectively. For homopolymer data see Figure 1. (◆) Peak overlap data sets, (◇) TTS data sets, (□) tracer contribution to η, and (○) tracer contribution to η'. PEO homopolymer data are added for comparison purposes.

solution with a Newtonian medium is to consider additivity:[47] $\eta_{blend} = \phi_{matrix}\eta_{matrix} + \phi_{tracer}\eta_{tracer}$. We have found eq 6 to be better at extracting the tracer monomeric friction factor. One might expect the parameter A to reflect the contribution of tracer−tracer contact to the overall blend viscosity. However,

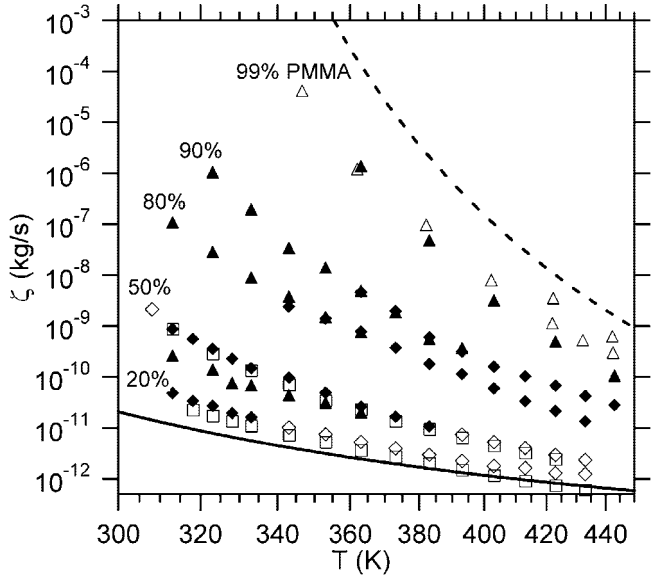

Figure 5. Monomeric friction factors of PEO in PEO/PMMA blends. Solid and dashed lines are PEO and PMMA homopolymer WLF fits, respectively. For homopolymer data see Figure 1. (◆) Peak overlap data sets, (◇) TTS data sets, (□) tracer contribution to η, (▲) FRS data, and (△) literature FRS data shifted by 17.5 K to account for T_g differences.[7] PMMA homopolymer data are added for comparison purposes.

the negative parameter values indicate that the additivity rule actually overestimates η_{blend}.

Extracting ζ via the Real Component of the Complex Shear Viscosity. When we consider the real component of the complex shear viscosity in Figure 2, we see that it exhibits two plateaus: one at low frequencies and another at higher frequencies. The transition occurs at the frequency that corresponds to the relaxation peak of the tracer chains in η''. If we relate the difference between the plateau values to the contribution of the tracer chains, then we may formulate a simple relation in conjunction with eq 6:

$$\eta'_{blend} = \phi_{matrix}\eta'_{matrix} + (\phi_{tracer} + A\phi_{tracer}^2)\eta'_{tracer} \quad (7)$$

Here, η'_{blend} and η'_{matrix} are the low- and high-frequency plateau values, respectively. The latter is taken to be the value of η' at the same frequency at which η'' reaches a minimum. The sole exception to this is the PMMA in 50% PMMA value (Figure 2a), taken at the maximum angular velocity (ω) available, as no η'' minimum is visible. The value of the parameter A is the same as in eq 6. We extracted η'_{tracer} from eq 7 and used the Rouse prediction (eq 4 with the rhs divided by 3 and with η' in place of η, which is valid at frequencies that correspond to $\omega\tau_1 \ll 1$[47]) to obtain the monomeric friction factor of the tracer. As before, we use the matrix density in eq 4, but all other parameters are the tracer parameters. This procedure yields data that are not in such good agreement with those extracted using the previous methods. A possible reason for this is the modification of matrix dynamics due to the presence of the tracer. We then use an Einstein-type equation to account for this effect:[51]

$$\eta'_{matrix,apparent} = \eta'_{matrix}(1 + B\phi_{tracer}) \quad (8)$$

Using eqs 8 and 7 simultaneously, the data extracted agree very well with those obtained via the previous methods when $B_{PMMA} = 10$ (Figure 4). As with the case of steady shear viscosity, we found the combination of eqs 7 and 8 to be better at extracting ζ_{tracer} than the simple additivity assumption.

Effect of the PEO Hydroxyl End Groups on Blend Dynamics. Sample PEO-1, used as the matrix PEO component, is an α,ω-hydroxy-terminated polymer. This raises the pos-

sibility that these hydroxyl groups might act as hydrogen bond donors, interacting either with the PMMA carbonyl oxygen or with the PEO ether oxygen, which might impact the relaxation of either the tracer or the matrix. Using thermal analysis, it has been shown that hydroxyl end groups do exert a measurable effect on the enthalpy of mixing of low molecular weight analogues of PMMA and PEO. Tetraethylene glycol with two, one, and no hydroxyl end groups were mixed with methyl isobutyrate (MIB), and the interaction parameter became increasingly positive with an increase in the number of hydroxyl end groups.[52] These effects were attributed to favorable self-interaction among the hydroxyl end groups vs cross-interaction with MIB. We do not expect the end groups to contribute appreciably to the blend dynamics because the mole ratio of hydrogen bond donor to acceptor, regardless of the identity of the latter, is small for compositions $\phi_{PMMA} > 0.1$. However, it is certainly worthwhile to check the influence of the end groups on the dynamics of the blends. To this end, the monomeric friction factor of sample PEO DME-1 was obtained at various temperatures via the pure homopolymer melt viscosity (divided by 3). In addition, PMMA-100 was blended with PEO DME-1, and the PMMA ζ was extracted via tracer contribution to η. We use the literature value $T_{g,PEO\ DME} = 187$ K,[53] where $T_{g,i}$ is the glass transition temperature of species i. Allowing for the difference in T_g values by considering ζ vs $T - T_g$ (plot not shown), the PEO and PEO DME monomeric friction factors overlap. Moreover, ζ values of the 1% PMMA tracer in PEO DME overlap with those of the host matrix, just as ζ of the 1% PMMA tracer in PEO do. Consequently, at this stage there is no indication that the hydroxyl end groups significantly affect the dynamics of either component in the blend for PEO $M_w \geq$ 1 kDa.

Discussion

Reliability of Results. In order to establish the reliability of the data obtained via the several methods previously detailed, they need to be compared to each other, to data obtained using other methods, and to literature data. Figure 1 shows good agreement among the four methods and literature data for the pure homopolymer melts.[4,9,13,48,50] At first glance, it may appear that the PEO data in Figure 1b do not agree well. However, since the accessible temperature window is far above T_g, the data span about 1.5 decades (vs 6.5 decades in Figure 1a) and never deviate by more than a factor of 2. For a low-modulus, low-viscosity sample such as PEO-1, we consider the data in Figure 1b to agree well.

Most importantly, Figures 4 and 5 show good agreement among the data obtained via the four methods for various blend compositions. This further supports the validity of the data and shows that these methods are not limited to mixing tracer chains in matrices of the same chemical species. Forced Rayleigh scattering results were obtained for optically labeled PEO chains in various blend compositions. As seen from Figure 5, the results agree very well with the 80% and 90% PMMA rheology results. There is, however, some discrepancy at 50% PMMA. The molecular weights of the tracers used in the rheological and FRS methods are very different (900K and 1K PEO, respectively). In light of this fact, the agreement between the FRS and mechanical data lends significant support to the overall validity of the analysis. At 50% PMMA, the 1 kDa PEO optical tracer relaxes very quickly, and fitting eq 1 to the resultant FRS decay curve might result in error, as the short-time plateau is missing. We tentatively attribute the discrepancy between the 50% blend FRS and rheology data to this fast decay. Indeed, the PEO friction factors extracted from these FRS data sets point to a faster relaxing chain than the rheology data suggest.

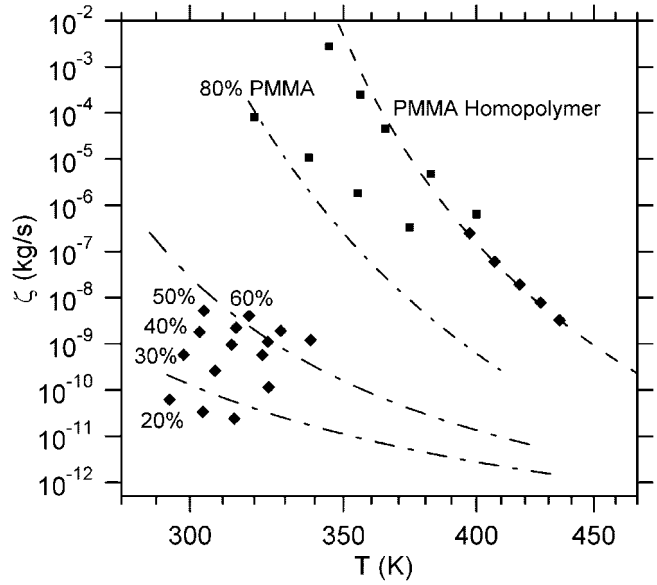

Figure 6. Comparison between Zawada et al.'s data[13] (◆, shifted by −51 deg; PMMA T_g 401 K), Colby's data[4] (■, shifted by −73 deg; PMMA T_g 402 K), and our data (dashed line is our homopolymer WLF fit; dash-dot lines are WLF fits to our PMMA data in 20, 50, and 80% PMMA; pure PMMA T_g 329 K).

Having established overall agreement among the various rheological methods, as well as with FRS and homopolymer literature data, we turn to literature data for PMMA terminal dynamics in blends of varying composition (Figure 6).[4,13] In order to form a basis for comparison, literature data were shifted along the temperature axis to achieve overlap between the homopolymer data. Zawada et al.'s data, obtained via simultaneous flow birefringence and infrared dichroism following a linear step strain, agree with our data well. The agreement with Colby's data is not quite as satisfactory.

Dependence of Tracer Dynamics on Matrix Molecular Weight. It has been shown that the diffusion coefficient of high molecular weight 1,4-polybutadiene in low molecular weight matrices of the same species varies significantly with matrix molecular weight at 5 and 10 wt %.[23] The blends were entangled, albeit barely. In the present work, when extracting component dynamics via the relaxation peaks of the tracer chains, the molecular weights of the matrix components were not included in the calculations (eq 5). However, when extracting component dynamics via the tracer contribution to η and η', the molecular weight dependent matrix contributions to η and η' were included (eqs 6–8). The agreement between the various methods, and the fact that one method does not account for matrix molecular weight while the other two methods do, suggests that any dependence of our methods on the matrix molecular weight may be insignificant or is captured in the constants A and B in eqs 6–8. However, this issue merits further investigation, and results with different PMMA matrix molecular weights will be obtained in the future.

Composition Dependence of the Component Monomeric Friction Factors. Both PMMA and PEO monomeric friction factors increase monotonically upon reduction in temperature and, upon addition of PMMA, the slower component. The PMMA monomeric friction factor drops considerably upon addition of a small fraction of PEO, whereas PEO is not so strongly affected by the presence of PMMA. The exception to this behavior arises when increasing the PMMA above 90%; the PEO monomeric friction factor then increases significantly.

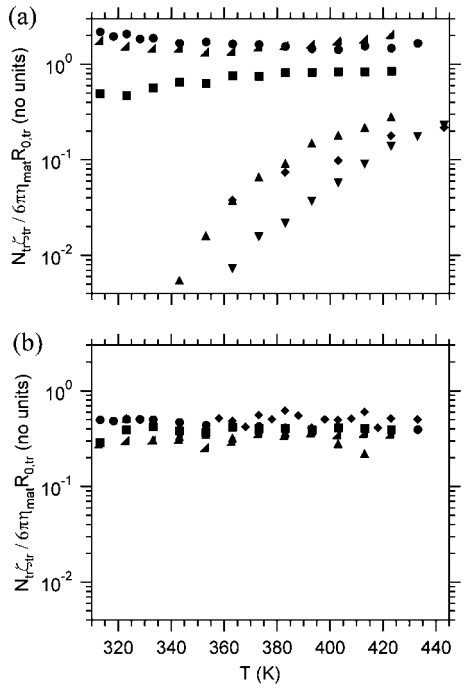

Figure 7. Ratio of chain friction coefficients to matrix viscosity (a) PEO and (b) PMMA: (tilted ▲) 0% PMMA, (●) 20% PMMA, (■) 50% PMMA, (▲) 80% PMMA, (▼) 90% PMMA, and (◆) 100% PMMA.

The overall trends are perfectly reasonable; all friction factors increase with decreasing temperature at fixed composition and with increasing high-T_g component at fixed temperature.

Dilute Tracers in Homopolymer Matrices. Two interesting phenomena emerge from tracers of one species in a pure matrix of the other species. First, ζ_{PMMA} in PEO assumes the value of the host matrix, ζ_{PEO}. In fact, both friction factors have the same temperature dependence and very nearly the same values for $\phi_{PMMA} \leq 0.2$. In contrast, ζ_{PEO} in pure PMMA is much smaller than that of the host matrix. The motion of the PMMA tracer chains in PEO is not dynamically restricted by the surrounding matrix as it is in the PMMA homopolymer melt. Because PEO relaxes so much more rapidly, PMMA can change conformations at a rate that is unimpeded by the surroundings. A PEO tracer in PMMA experiences less friction than that associated with the host matrix. These results imply that PEO can relax via conformation changes that do not depend on the surrounding matrix. To some extent, these results are consistent with a simple picture in which PMMA is the solute and PEO is the solvent. In dilute solution, the polymer (PMMA) friction tracks the solvent (PEO) viscosity, whereas at high polymer concentration the solvent (PEO) relaxes more rapidly than the polymer (PMMA) segments.

To pursue this idea further, the tracer component friction factors, multiplied by N_{tracer}, are normalized to the matrix viscosity, multiplied by $6\pi R_0$, across the full composition range, as shown in Figure 7; R_0 is the end-to-end distance of the tracer chains. Overall, the PMMA friction factors track the matrix viscosity rather well over the entire composition range (Figure 7b). In contrast, Figure 7a shows that for blends with 80% PMMA or more the PEO ratio drops considerably as the temperature is lowered, suggesting that the mobility of the PEO chains is much less affected by the drop in temperature than the viscosity of the PMMA-rich matrix. It is for the same blends that TTS fails over the entire accessible temperature range, as noted in Figure 3d,e. This suggests there may be a qualitative change in the mechanism of PEO relaxation under these conditions.

Comparison of Segmental and Terminal Data. The PEO terminal data in Figure 5 are in strong disagreement with published PEO segmental data.[9,50] Though the PEO monomeric friction factor, as obtained via terminal measurements, is not as significantly affected by the presence of PMMA as vice versa, its composition dependence is notably steeper than that of the segmental data. The reasons for this apparent decoupling of terminal and segmental data are unclear at this time. A possible explanation for this phenomenon is that segmental dynamics measurements are actually evaluating a correlation function that is unassociated or weakly associated with the long time relaxation of the segment. We cannot, however, ignore the agreement that these measurement schemes have enjoyed with terminal dynamics measurements in numerous other blends, most notably PI/PVE.[21]

Comparison with the Lodge−McLeish Model. The Lodge−McLeish model has been found to describe the segmental dynamics of PEO in PMMA blends, albeit with a self-concentration (ϕ_s) value larger than anticipated.[9] The model also fits PEO segmental data published elsewhere,[50] but only for PEO rich blends and very small values of ϕ_s. Given that the terminal dynamics data here differ from these segmental results, we may expect that the model will not be successful in fitting our results. It has been reported[48] that the self-concentration model is unable to describe Zawada et al.'s terminal PMMA dynamics[13] but is capable of fitting Colby's data.[4] The self-concentration model is simple to implement. One begins with the WLF function describing the homopolymer data and then adjusts the glass transition temperature using the Fox relation (or other mixing rule for T_g) and the effective local concentration associated with a chosen value of ϕ_s. As can be seen in Figure 8, this model cannot predict the data reported here, even for values of ϕ_s approaching zero. The friction factors of PMMA (Figure 8a) lie consistently below, whereas those of PEO (Figure 8b) lie above the $\phi_s = 0$ curves. This indicates that the PMMA dynamics are accelerated by the addition of PEO more than one would expect based on the Fox relation and without accounting for any local enhancement due to chain connectivity. Similarly, the PEO is retarded by PMMA more than the Fox relation suggests.

Mixing Rule To Account for "Tribological Effects" in the Blend. The self-concentration approach does not consider explicitly any change in the mean friction experienced by a segment upon blending. Rather, it simply rescales the effective glass transition experienced by a chain, based on local average composition. In fact, all chains of species i in the blend experience $i-i$ and $i-j$ contacts, with corresponding probabilities for each type of contact. When segments i and j have such inherently different mobilities as in PEO/PMMA (or some polymer solutions), it may be necessary to account for this in some way. In the absence of more comprehensive theory, we propose an empirical mixing rule, based on an approach offered by several researchers.[16,55,56] Given that a chain of species i exists (probability ϕ_i), the probabilities for $i-i$ and $i-j$ contacts are $P_{i-i} = \phi_i\phi_i/\phi_i = \phi_i$ and $P_{i-j} = \phi_j\phi_i/\phi_i = \phi_j$, respectively. These probabilities assume that the presence of i is independent of the presence of i or j; i.e., no enthalpic effects are taken into consideration. The reason we choose the mean blend compositions rather than the effective concentrations for these probabilities is that the segment cannot come in contact with its adjoining segments on the chain in a manner that produces friction. This suggests an equation of the form

$$\log(\zeta_{i,b}) = \phi_i \log(\zeta_{i-i}) + \phi_j \log(\zeta_{i-j}) \quad (9)$$

where $\zeta_{i,b}$ is the monomeric friction factor of component i in the blend and ζ_{i-j} is the friction experienced by a segment of species i due to contacts with segments of species j. We propose

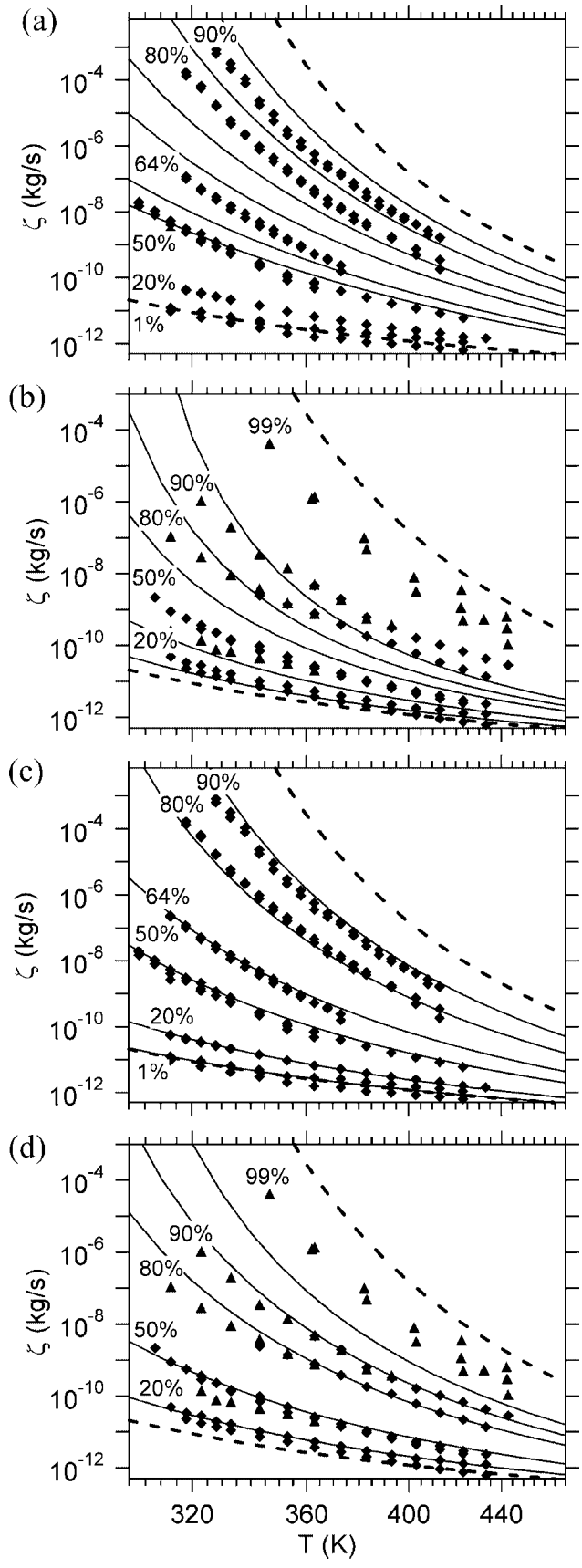

Figure 8. Lodge−McLeish predictions for (a) PMMA and (b) PEO with $\phi_{s,PEO} = \phi_{s,PMMA} = 0$. Modified mixing rule predictions ($\phi_{s,PEO} = 0.57$,[48] $\phi_{s,PMMA} = 0.25$[10]) for (c) PMMA with $\alpha_{PMMA} = -0.3\phi_{PMMA}$ and (d) PEO with $\alpha_{PEO} = 0.45$. Thick dashed lines are homopolymer WLF fits.[54] (◆) All rheological data. (▲) All FRS data, whether obtained from this work or from the literature.[7] Percentages shown pertain to PMMA content. The parameter α is defined in the text.

Table 2. Comparison of Various Values of α_i in Eq 10 and Their Implications

α_i	ζ_{i-j}	eq *10*	implication	notes
1	$\zeta_{i-j} = \zeta_{i-i}$	$\zeta_{i,b} = \zeta_{i,h\ L-M}$	$i-j$ contact is characterized by the i species contact friction	result of Lodge−McLeish; blending only affects component's reference WLF temperature
0	$\zeta_{i-j} = \zeta_{j-j}$	$\log \zeta_{i,b} = \phi_i \log \zeta_{i,h\ L-M} + \phi_j \log \zeta_{j,h\ L-M}$	$i-j$ contact is characterized by the j species contact friction	prediction for both species is exactly the same; result of blends of 20% PMMA and lower
$-\phi_i/\phi_j$		$\zeta_{i,b} = \zeta_{j,h\ L-M}$	negative α_i indicates that a component's dynamics are strongly affected by the presence of the second species, both tribologically and free volume wise	behavior typical of slow components in many blends; plasticizing effect of the fast component dominates dynamics even when the fast component fraction in the blend is small

a general correlation $\zeta_{i-j} = \zeta_{i-i}^{\alpha_i}\zeta_{j-j}^{1-\alpha_i}$, where ζ_{i-i} and ζ_{j-j} may be given by the homopolymer friction factors, $\zeta_{i,h}$ and $\zeta_{j,h}$, shifted according to Lodge−McLeish. Then we obtain

$$\log(\zeta_{i,b}) = \phi_i \log(\zeta_{i,h\ L-M}) + \phi_j \log(\zeta_{j,h\ L-M}) + \alpha_i\phi_j \log(\zeta_{i,h\ L-M}/\zeta_{j,h\ L-M}) \quad (10)$$

Table 2 compares the results of various values of α_i.

Parts c and d of Figure 8 compare the predictions of eq 10 with the data. The model describes the PMMA terminal data remarkably well over the entire composition range (Figure 8c). The PEO data are also modeled well, except perhaps for the highest PMMA concentrations. The discrepancies at 80% and 90% PMMA content probably stem from intrachain relaxation mechanisms playing a more dominant role in PEO dynamics, as noted in the context of Figures 3d,e and 7. Interestingly, PEO tracer chains in PMMA, on the other hand, relax more slowly than expected by the mixing rule.

In addition to the relative success that this model enjoys for PEO/PMMA blends, it successfully predicts the published terminal results of PI and PS in their respective blends using $\phi_{s,PS} = 0.42$, $\phi_{s,PI} = 0.33$, and $\alpha_{PS} = \alpha_{PI} = -0.25$.[8] It also improves the PVE predictions in PI/PVE blends using $\phi_{s,PI} = 0.4$, $\phi_{s,PVE} = 0.2$, and $\alpha_{PVE} = 1.7$.[21] The value of α being greater than unity is problematic, and indeed the predictions are still not satisfactory. As for PI, the self-concentration model predicts its dynamics well, so $\alpha_{PI} = 1$.

Summary

High molecular weight tracer chains of either PEO or PMMA have been blended with low molecular weight matrices of various compositions. Homopolymer friction factors have been obtained from the steady shear viscosity. For the blends, the η', η'', and η material functions have been obtained, and three methods have been devised to extract terminal component dynamics: The longest relaxation times of the tracer chains are apparent via η'' peaks. The presence of the tracer chains enhances the blend steady shear viscosity. We employed a simple formulation to extract the contribution of the tracer chains to η. We then used the Rouse model to extract component ζ values. Lastly, concurrent with the η'' relaxation peaks of the

tracer chains, η' plateau values shift to reflect the fact that the stress in the sample is sustained via different mechanisms once the tracer chains relax. Using the same formulation as that used to extract tracer contribution to η, we obtain the tracer contribution to η'. In addition, we used an Einstein-type equation to account for the modification of the matrix η' value due to the presence of the tracer chains. The results obtained agree well with each other as well as with most literature data and FRS results obtained for PEO.

Selected experiments were repeated using PEO−DME, thereby eliminating any hydrogen bonding. We obtain equivalent results, except for a shift in T_g. This indicates that hydrogen bonds do not contribute significantly to the blend dynamics at PEO molecular weights ≥1 kDa.

The PMMA mobility increases dramatically upon addition of a small fraction of PEO. As the matrix becomes richer in PEO, PMMA mobility increases more moderately, until in a pure PEO matrix the PMMA friction factors coincide with those of the PEO. The PEO mobility is not as strongly affected by the presence of PMMA until the matrix becomes PMMA-rich ($\phi_{PMMA} \geq 0.9$). At these compositions, the PEO mobility also becomes significantly dependent on composition. The mobility of PEO tracer chains in a 100% PMMA matrix, however, does not assume the matrix values.

The Lodge−McLeish model does not describe the data well for either component. An empirical mixing rule, however, is able to fit the experimental results. This mixing rule incorporates two concepts: shifting the homopolymer WLF curves to account for glass transition changes upon blending, as in the Lodge−McLeish model, and "mixing" these shifted curves to account for specific effects of nearest neighbors on mobility. The model includes one new parameter that determines the relative weight of $i-i$ and $j-j$ contacts in accounting for the effect of $i-j$ contacts.

Acknowledgment. This work was supported by the National Science Foundation through Award DMR-040656. We also thank Dr. Jeff Haley and Dr. Hiroshi Watanabe for insightful discussions.

Supporting Information Available: Viscoelastic properties of the low molecular weight PEO and PMMA matrix polymers and their blends and DSC traces of the same materials. This material is available free of charge via the Internet at http://pubs.acs.org.

References and Notes

(1) Chung, G. C.; Kornfield, J. A.; Smith, S. D. *Macromolecules* **1994**, *27*, 5729–5741.
(2) Lau, S.-F.; Pathak, J. A.; Wunderlich, B. *Macromolecules* **1982**, *15*, 1278–1283.
(3) Lodge, T. P.; Wood, E. R.; Haley, J. C. *J. Polym. Sci., Part B: Polym. Phys.* **2006**, *44*, 756–763.
(4) Colby, R. H. *Polymer* **1989**, *30*, 1275–1278.
(5) Pathak, J. A.; Colby, R. H.; Floudas, G.; Jerome, R. *Macromolecules* **1999**, *32*, 2553–2561.
(6) Cavaille, J. Y.; Perez, J.; Jourdan, C.; Johari, G. P. *J. Polym. Sci., Part B: Polym. Phys.* **1987**, *25*, 1847–1858.
(7) Haley, J. C.; Lodge, T. P. *J. Chem. Phys.* **2005**, *122*, 234914.
(8) He, Y.; Lutz, T. R.; Ediger, M. D.; Pitsikalis, M.; Hadjichristidis, N.; von Meerwall, E. D. *Macromolecules* **2005**, *38*, 6216–6226.
(9) Lutz, T. R.; He, Y.; Ediger, M. D.; Cao, H.; Lin, G.; Jones, A. A. *Macromolecules* **2003**, *36*, 1724–1730.
(10) Lodge, T. P.; McLeish, T. C. B. *Macromolecules* **2000**, *33*, 5278–5284.
(11) Ito, H.; Russell, T. P.; Wignall, G. D. *Macromolecules* **1987**, *20*, 2213–2220.
(12) Fernandes, A. C.; Barlow, J. W.; Paul, D. R. *J. Appl. Polym. Sci.* **1986**, *32*, 5481–5508.
(13) Zawada, J. A.; Ylitalo, C. M.; Fuller, G. G.; Colby, R. H.; Long, T. E. *Macromolecules* **1992**, *25*, 2896–2902.
(14) Wang, C. H.; Zhang, X. Q.; Fytas, G.; Kanetakis, J. *J. Chem. Phys.* **1989**, *91*, 3160–3167.
(15) Xia, J. L.; Wang, C. H. *J. Chem. Phys.* **1991**, *94*, 3229–3234.
(16) Wu, S. *J. Polym. Sci., Part B: Polym. Phys.* **1987**, *25*, 2511–2529.
(17) Lumma, D.; Borthwick, M. A.; Falus, P.; Lurio, L. B.; Mochrie, S. G. J. *Phys. Rev. Lett.* **2001**, *86*, 2042–2045.
(18) Booij, H. C.; Palmen, J. H. M. In *International Congress on Rheology*; Moldenaers, P., Keunings, R., Eds.; Elsevier Science Publishers, B.V.: Brussels, Belgium, 1992; pp 321−323.
(19) Yang, X.; Halasa, A.; Hsu, W.-L.; Wang, S.-Q. *Macromolecules* **2001**, *34*, 8532–8540.
(20) Shams Es-Haghi, S.; Yousefi, A. A.; Oromiehie, A. *J. Polym. Sci., Part B: Polym. Phys.* **2007**, *45*, 2860–2870.
(21) Haley, J. C.; Lodge, T. P.; He, Y.; Ediger, M. D.; von Meerwall, E. D.; Mijovic, J. *Macromolecules* **2003**, *36*, 6142–6151.
(22) Alegria, A.; Colmenero, J.; Ngai, K. L.; Roland, C. M. *Macromolecules* **1994**, *27*, 4486–4492.
(23) Wang, S.; von Meerwall, E. D.; Wang, S.-Q.; Halasa, A.; Hsu, W.-L.; Zhou, J. P.; Quirk, R. P. *Macromolecules* **2004**, *37*, 1641–1651.
(24) Roland, C. M.; Ngai, K. L. *Macromolecules* **1991**, *24*, 2261–2265.
(25) Roovers, J.; Toporowski, P. M. *Macromolecules* **1992**, *25*, 3454–3461.
(26) Roovers, J.; Toporowski, P. M. *Macromolecules* **1992**, *25*, 1096–1102.
(27) Liu, C. Y.; Halasa, A. F.; Keunings, R.; Bailly, C. *Macromolecules* **2006**, *39*, 7415–7424.
(28) Lee, J. H.; Fetters, L. J.; Archer, L. A.; Halasa, A. F. *Macromolecules* **2005**, *38*, 3917–3932.
(29) Tsenoglou, C. *New Trends Phys. Phys. Chem. Polym., [Proc. Int. Symp.]* **1989**, *375*, 383.
(30) Des Cloizeaux, J. *Europhys. Lett.* **1988**, *5*, 437–442.
(31) Haley, J. C.; Lodge, T. P. *J. Rheol.* **2004**, *48*, 463–486.
(32) Ndoni, S.; Papadakis, C. M.; Bates, F. S.; Almdal, K. *Rev. Sci. Instrum.* **1995**, *66*, 1090–1095.
(33) Wiles, D. M.; Bywater, S. *Trans. Faraday Soc.* **1965**, *61*, 150–158.
(34) Allen, R. D.; Long, T. E.; McGrath, J. E. *Polym. Bull.* **1986**, *15*, 127–134.
(35) Hadjichristidis, N.; Latrou, H.; Pispas, S.; Pitsikalis, M. *J. Polym. Sci., Part A: Polym. Chem.* **2000**, *38*, 3211–3234.
(36) Gilman, H.; Cartledge, F. K. *J. Organomet. Chem.* **1964**, *2*, 447–454.
(37) Gomez-Anton, M. R.; Horta, A.; Hernandez-Fuentes, I. *Polym. Commun.* **1986**, *27*, 5.
(38) Spickermann, J.; Martin, K.; Räder, H. J.; Müllen, K.; Schlaad, H.; Müller, A. H. E.; Kruger, R. P. *Eur. J. Mass Spectrom.* **1996**, *2*, 161–165.
(39) Pham, Q. T.; Petiaud, R.; Waton, H.; Llauro-Darricades, M.-F. *Proton and Carbon NMR Spectra of Polymers*; Penton Press: London, 1991.
(40) Varshney, S. K.; Hautekeer, J. P.; Fayt, R.; Jerome, R.; Teyssie, P. *Macromolecules* **1990**, *23*, 2618–2622.
(41) Liau, W. B.; Chang, C. F. *J. Appl. Polym. Sci.* **2000**, *76*, 1627–1636.
(42) Huang, W. J.; Frick, T. S.; Landry, M. R.; Lee, J. A.; Lodge, T. P.; Tirrell, M. *AlChE J.* **1987**, *33*, 573–582.
(43) Rouse, P. E. *J. Chem. Phys.* **1953**, *21*, 1272–1280.
(44) Ferry, J. D. *Viscoelastic Properties of Polymers*, 3rd ed.; John Wiley & Sons: New York, 1980.
(45) Fetters, L. J.; Lohse, D. J.; Richter, D.; Witten, T. A.; Zirkel, A. *Macromolecules* **1994**, *27*, 4639–4647.
(46) Inoue, T.; Okamoto, H.; Osaki, K. *Macromolecules* **1991**, *24*, 5670–5675.
(47) Doi, M.; Edwards, S. F. *The Theory of Polymer Dynamics*; Clarendon Press: New York, 1986.
(48) He, Y.; Lutz, T. R.; Ediger, M. D. *J. Chem. Phys.* **2003**, *119*, 9956–9965.
(49) Milhaupt, J. M.; Lodge, T. P.; Smith, S. D.; Hamersky, M. W. *Macromolecules* **2001**, *34*, 5561–5570.
(50) Lartigue, C.; Guillermo, A.; Cohen-Addad, J. P. *J. Polym. Sci., Part B: Polym. Phys.* **1996**, *35*, 1095–1105.
(51) Morris, R. L.; Amelar, S.; Lodge, T. P. *J. Chem. Phys.* **1988**, *89*, 6523–6537.
(52) Min, K. E.; Chiou, J. W.; Barlow, J. W.; Paul, D. R. *Polymer* **1986**, *28*, 1721–1728.
(53) Blazejczyk, A.; M. Szczupak, M.; Wieczorek, W.; Cmoch, P.; Appetecchi, G. B.; Scrosati, B.; Kovarsky, R.; Golodnitsky, D.; Peled, E. *Chem. Mater.* **2005**, *17*, 1535–1547.
(54) Williams, M. L.; Landel, R. F.; Ferry, J. D. *J. Am. Chem. Soc.* **1955**, *77*, 3701–3707.
(55) Brochard-Wyrat, F. *C. R. Acad. Sci. Paris* **1987**, *305*, 657–660.
(56) Chapman, B. R.; Hamersky, M. W.; Milhaupt, J. M.; Kostelecky, C.; Lodge, T. P.; von Meerwall, E. D.; Smith, S. D. *Macromolecules* **1998**, *31*, 4562–4573.

MA0709809